CrossMark

ORIGINAL PAPER

Properties of low-density polyethylene/natural rubber/water hyacinth fiber composites: the effect of alkaline treatment

S. J. Tan[1,2] · A. G. Supri[1]

Abstract The effect of alkaline treatment on the properties of low-density polyethylene/natural rubber/water hyacinth fiber (LDPE/NR/WHF) composites was studied. LDPE/NR/WHF and LDPE/NR/WHF$_{NaOH}$ composites were prepared using a Brabender Plasticorder. The LDPE/NR/WHF$_{NaOH}$ composites showed higher tensile strength, Young's modulus, and melting temperature (T_m) but lower molar sorption and interparticle spacing (d) than did the LDPE/NR/WHF composites. Fourier transform infrared spectroscopy (FTIR) results confirmed that alkaline treatment removed hemicellulose and lignin in WHF, as evidenced by the disappearance of the absorption bands at 1732.79 and 1250.91 cm^{-1}. The LDPE/NR/WHF$_{NaOH}$ composites demonstrated less thermal stability and rougher surface after alkaline treatment.

Keywords Low-density polyethylene · Natural rubber · Alkaline treatment · Water hyacinth fibers

Introduction

Over the recent years, natural fibers such as kenaf, bagasse, jute, ramie, hemp, oil palm, coir, bamboo, and wood, have gained extensive research attention because of their advantages over synthetic fibers. Natural fibers used as reinforcement in thermoplastic or thermoset polymers yield products with lower density, higher

✉ S. J. Tan
  sjtan@unimap.edu.my

1 Faculty of Engineering Technology, Universiti Malaysia Perlis (UniMAP), P.O Box 77, D/A Pejabat Pos Besar, 01000 Kangar, Perlis, Malaysia

2 Center of Excellence Geopolymer and Green Technology, School of Materials Engineering, Universiti Malaysia Perlis (UniMAP), P.O Box 77, D/A Pejabat Pos Besar, 01007 Kangar, Perlis, Malaysia

specific stiffness, and less machine wearing than those produced through mineral reinforcement; moreover, natural fibers do not present any health hazards, demonstrate high degree of flexibility, and are widely available from natural resources [1].

Water hyacinth (*Eichhornia crassipes*) is a productive aquatic macrophyte found throughout tropical and subtropical regions worldwide [2]. This macrophyte is supplied to many gardeners and horticulture practitioners because of its attractive blue, lilac, or purplish flowers and round-to-oval leaves [3]. Nevertheless, water hyacinth presents several limitations, such as rapid mat turnover and high-density growth, which may clog water bodies and, in turn, confers negative effects on the environment, human health, and economic development [4–6]. Opande et al. [7] reported a massive accumulation of water hyacinth biomass in many beaches and bays of Winam gulf because of the rapid reproduction rate of this plant.

Patel et al. [8] chemically analyzed water hyacinth and found that it contains high amounts of cellulose and hemicellulose, which are about 17.8 and 43.4 %, respectively. With the high cellulose and hemicellulose contents of water hyacinth, the plant exhibits potential as reinforced fiber in thermoset and thermoplastic composites. Mantia et al. [9] studied the addition of organic fillers to recycled post-consumer polyethylene and found that the treatment enhanced elastic modulus (stiffness) and thermo-mechanical resistance. Holbery and Houston [10] further reviewed the potential of natural fiber reinforced with polymer composites in numerous automotive interior and exterior parts.

Fiber modification is required to improve the mechanical properties of polymer composites, which lack good adhesion between natural fibers and polymeric matrix. The hydrophilic nature of natural fibers could adversely affect adhesion to a hydrophobic matrix and result in loss of strength [1]. Several modification methods developed include alkaline treatment, grafting with maleic anhydride copolymer, use of silane coupling agent, acetylation, etherification, benzoylation, and isocyanate treatment on natural fibers [11].

Alkaline treatment or mercerization is one of the most applied chemical treatments for natural fibers when reinforced with thermoplastic and thermoset composites. Alkaline treatment increases the amount of amorphous cellulose at the expense of crystalline cellulose. An important aspect of natural fiber modification using alkaline treatment is the removal of hydrogen bonding in the network structure. The following reaction proceeds as a result of alkaline treatment [12]:

$$\text{Fiber-OH} + \text{NaOH} \rightarrow \text{Fiber-O-Na}^+ + \text{H}_2\text{O}$$
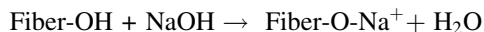
Several authors have studied alkaline treatment on natural fibers and characterized changes in fiber properties. Bisanda and Ansell [13] discussed that alkaline treatment improved the resin pick-up or wettability of the fibers, as evidenced by increased composite density; they believed that the treatment improved the interfacial bonding by increasing the number of additional sites for mechanical interlocking, hence promoting resin/fiber interpenetration at the interface.

Goswami et al. [14] determined the influence of sodium hydroxide (NaOH) treatment on the optical and structural properties of cellulose; the results showed

that NaOH changed the density, crystallinity, pore structure, and fibril orientation of cellulosic fibers. Gwon et al. [15] showed that wood fibers treated with NaOH in a polypropylene matrix presented enhanced physical properties compared with composites with untreated fibers. The impurities of wood fibers were eliminated by NaOH, thereby improving the adhesion between fibers and PP matrix.

In this study, the effect of alkaline treatment on water hyacinth fibers (WHF) on mechanical properties, molar sorption, FTIR analysis, thermal properties, thermal degradation analysis and X-ray diffraction (XRD) characteristics was investigated in low-density polyethylene/natural rubber/water hyacinth fiber (LDPE/NR/WHF) composites.

Experimental

Materials

Fresh WHFs were obtained from Local River in Perlis, Malaysia. LDPE pellets (density = 0.91–0.94 g/cm^3, processing temperature = 134–210 °C, melting temperature = 98–115 °C, and melt flow index = 0.26) were supplied by Mega Makmur Sdn. Bhd., Penang, Malaysia. NR (SMR-L) was purchased from Rubber Research Institute Malaysia. NaOH (molecular weight = 40 g/mol) was supplied by HmbG Chemicals. Ethanol (95 vol.%, C_2H_5OH, molecular weight = 46.07 g/mol) was purchased from HmbG Chemicals, and toluene ($C_6H_5CH_3$) was obtained from AR Alatan Sdh. Bhd., Alor Star, Kedah, Malaysia.

Preparation of water hyacinth fibers

Fresh water hyacinth stems were cleaned with water to remove dust and ash. The stems were cut into small pieces and then dried in an oven at 105 °C for 8 h to evaporate all water content. The dried water hyacinth was ground into powder and designated as water hyacinth fiber (WHF). After sieving, fibers, with an average particle size of 63 μm, were selected.

Alkaline treatment on water hyacinth fibers

WHFs, with an average particle size of 63 μm, were treated with 1 mol dm^{-3} NaOH solution and soaked at room temperature for 2 h. The treated WHFs were washed with distilled water for several times until the rinsing solution became neutral to remove the remaining NaOH on the fiber surface. The pH of the treated fibers was 7, as determined by universal indicator paper. The treated fibers were dried in the oven at 70 °C for 24 h to remove moisture.

Composites preparation

The composites were compounded using a Brabender Plasticorder. LDPE/NR/WHF and LDPE/NR/WHF$_{NaOH}$ composites were prepared. The Brabender Plasticorder

Table 1 The formulation of LDPE/NR/WHF and LDPE/NR/WHF$_{NaOH}$ composites

Materials	LDPE/NR/WHF (phr)	LDPE/NR/WHF$_{NaOH}$ (phr)
LDPE	80	80
NR	20	20
WHF	5, 10, 15, 20, 25	–
WHF$_{NaOH}$	–	5, 10, 15, 20, 25

was set at 160 °C with a rotor speed of 50 rpm. LDPE pellets were loaded into the mixing chamber and preheated for 1 min. Afterwards, NR and WHFs were added into the softened LDPE matrix. The mixture was mixed for 5 min to obtain homogeneous composites. The softened composites were removed from the chamber and pressed into thick round pieces. The formulations of LDPE/NR/WHF and LDPE/NR/WHF$_{NaOH}$ composites are shown in Table 1.

Compression molding

A hydraulic hot press was used to produce composites in a plate form. The machine was set at 160 °C, both at the top and bottom plates. An empty mold was heated for 5 min. The composites were placed into the mold, preheated, and partially compressed for 10 min. After the composites started to soften, they were completely compressed for 6 min and cooled for 4 min.

Tensile test

Tensile test was conducted according to ASTM D638 by using Instron 5569 with a crosshead speed of 50 mm/min. Five dumbbell-shaped samples were used for each blend composition. Tensile strength, Young's modulus, and elongation at break were obtained from the test.

Swelling behavior test

The sorption of toluene through the blends was determined by the swelling behavior test. Three samples with a dimension of 20 mm × 10 mm × 10 mm were used for each blend composition. The samples were totally immersed in toluene for 46 h. After immersion, the samples were wiped with tissue paper and weighed using an analytical balance with 0.1 mg resolution. The molar sorption, Q_t of toluene by the samples after 46 h of immersion was calculated with:

$$Q_t = \frac{W_2 - W_1}{W_1 \times M_w} \times 100 \%\tag{1}$$

where Q_t is the molar sorption, W_1 is the weight of dried sample, W_2 is the weight of sample after immersion and M_w is the molecular weight of toluene.

Scanning electron microscopy (SEM)

The morphologies of the untreated WHF and NaOH-treated WHF, as well as the tensile fracture surfaces of the composites, were studied using a scanning electron microscope (SEM, model JOEL JSM-6460LA). Prior to the SEM examination, the samples were mounted on aluminum stubs and then sputter coated. A thin gold layer of 20 nm was sputter coated on the sample surface to avoid electrostatic charges during examination.

ATR–FTIR spectroscopy

Spectra were obtained using a PerkinElmer Spectrum 400 Series equipment. The spectrum resolution and the scanning range were set at 4 and 650–4000 cm^{-1}, respectively. FTIR spectra with percent transmittance (%T) versus wavelength (cm^{-1}) were obtained after scanning.

Differential scanning calorimetry

Thermal analysis measurements of the selected system were performed using a PerkinElmer differential scanning calorimeter (DSC-7 analyzer). Samples of about 4 mg were heated from 25 to 200 °C under a nitrogen airflow of 50 ml/min and a heating rate of 10 °C/min. The melting and crystallization behavior of the selected composites was analyzed. The crystallinity of the composites was determined using the following equation:

$$\% \, \text{Crystallinity} = \frac{\Delta H_f}{\Delta H_f^{\circ}} \times 100 \, \%$$ (2)

where ΔH_f and ΔH_f° are the enthalpy of fusion of the composite and standard enthalpy of fusion of LDPE, respectively. The value for ΔH_f° (LDPE) is 293.6 J/g.

Thermogravimetric analysis (TGA)

Thermogravimetry analysis (TGA) of the LDPE/NR/WHF and LDPE/NR/WHF$_{\text{NaOH}}$ composites was conducted using a PerkinElmer Pyris 6 TGA analyzer. Samples of about 10 mg were scanned from 30 to 600 °C with a heating rate of 10 °C/min under a constant nitrogen gas flow of 50 ml/min to prevent thermal oxidation. Temperature at 1 % ($T_{-1\%\text{wt}}$) and 50 % weight loss ($T_{-50\%\text{wt}}$), residual mass, and final decomposition temperature were calculated using the TGA curves.

X-ray diffraction (XRD) analysis

The XRD patterns of the composites were analyzed using a Shimadzu XRD-6000 Analyzer at an acceleration voltage of 35 kV and 25 mA with Cu Kα ($\lambda = 0.15406$ nm) radiation source. Scanning was conducted within the range of 10°–80° (2θ). Analysis was performed at ambient temperature with a scanning

speed of 5 °C/min. Bragg's Law was used to initially explain the X-ray interference through crystals and then to study the structures of different materials under wavelength comparable with the intermolecular space of the investigated material. Bragg's Law is presented as:

$$n\lambda = 2d\sin\theta \tag{3}$$

where d is the distance between atoms, n is the number of lengthways, λ is the wavelength of the incident radiation, and θ is the incident angle.

Results and discussion

Tensile properties

Figure 1 shows the effect of alkaline treatment on the tensile strength of the LDPE/NR/WHF and LDPE/NR/WHF$_{NaOH}$ composites at different amount of fibers. The tensile strength of both composites gradually increased as fiber loading increased from 5 to 20 phr and then decreased with further increase in fiber loading. The decrease of tensile strength at 25 phr was attributed to the poor dispersion of WHF in the LDPE/NR phases. With increasing amount of fibers added into the composites, fiber–fiber interaction, rather than fiber–matrix interaction, was promoted, resulting in weak fiber–matrix interaction. A fracture was initiated from the weak fiber–matrix interface during stress transfer from the matrix to the fibers, thereby reducing tensile strength. Karnani et al. [16] found that the efficiency of fiber-reinforced composites was dependent on the fiber–matrix interface and the capacity to transfer stress from the matrix to the fiber. Thus, stress-transfer efficiency plays a dominant role in determining the mechanical properties of the composites.

At similar fiber loading, the LDPE/NR/WHF$_{NaOH}$ composites yielded higher tensile strength than the LDPE/NR/WHF composites. This result was due to NaOH,
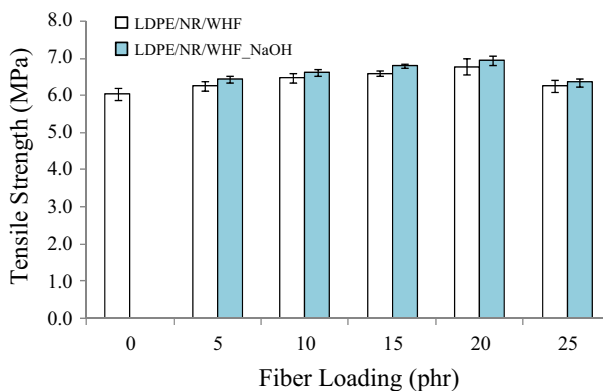

Fig. 1 The effect of alkaline treatment on tensile strength of LDPE/NR/WHF and LDPE/NR/WHF$_{NaOH}$ composites at different amount of fiber

which improved the surface roughness of the fibers and exposed cellulose on the fiber surface, thereby increasing the number of possible reaction sites [17]. The enhanced surface roughness of the fibers resulted in better interfacial adhesion between the fibers and the matrix. Bledzki and Gassan [18] reported that alkaline treatment on jute fibers removed lignin and hemicellulose; as such, the interfibrillar region could be less dense and rigid, resulting in increased capacity of fibrils to rearrange themselves along the direction of tensile deformation and increased tensile strength. In addition, Alawar et al. [19] reported that alkaline treatment induced fibers to be free from impurities and thus improved the tensile strength of the composites.

The effect of alkaline treatment on the Young's modulus of the LDPE/NR/WHF and LDPE/NR/WHF$_{NaOH}$ composites at different amount of fibers is shown in Fig. 2. The Young's modulus of the LDPE/NR/WHF and LDPE/NR/WHF$_{NaOH}$ composites significantly increased with increasing WHF content. This result was due to the strength and stiffness provided by the fibers to the composites. Carter [20] reported that the Young's modulus of the composites increased with increasing amount of fibers in the matrix. Figure 2 shows that the LDPE/NR/WHF$_{NaOH}$ composites exhibited higher Young's modulus than the LDPE/NR/WHF composites at similar fiber loadings. This observation was agreed with Threepopnatkul et al. [21], they reported that the Young's modulus of neat PC increased for composites with pineapple leaf treated with sodium hydroxide (PALF/NaOH/PC).

Figure 3 illustrates the effect of alkaline treatment on elongation at the breaks of the LDPE/NR/WHF and LDPE/NR/WHF$_{NaOH}$ composites at different amount of fibers. The elongation at break for both of the composites decreased while fiber loading increased. This might be due to the fibers obstructed which limited the chain mobility of the polymer matrix thus reduced the ductility of the composites. Similarly, Supri et al. [22] reported that fibers hardened and reduced the ductility of the composites. Comparison between untreated and NaOH-treated composites indicated that the LDPE/NR/WHF$_{NaOH}$ composites exhibited higher elongation at the break than the LDPE/NR/WHF composites at the same fiber loading. The
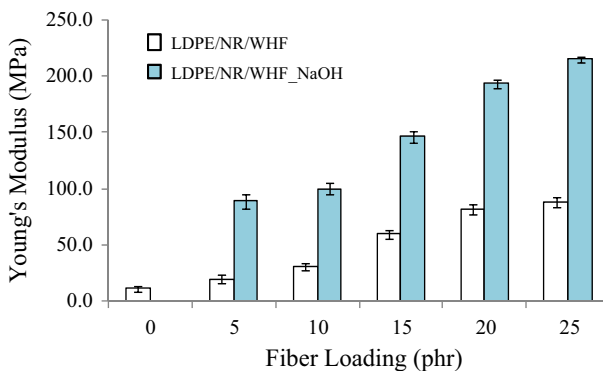

Fig. 2 The effect of alkaline treatment on Young's modulus of LDPE/NR/WHF and LDPE/NR/WHF$_{NaOH}$ composites at different amount of fiber
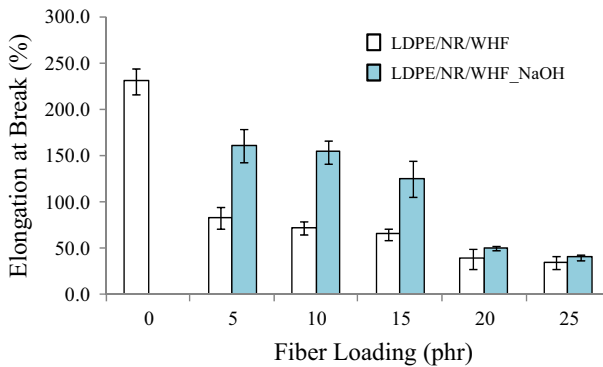
Fig. 3 The effect of alkaline treatment on elongation at break of LDPE/NR/WHF and LDPE/NR/WHF$_{NaOH}$ composites at different amount of fiber

removal of lignin, hemicellulose, and artificial impurities from WHF by NaOH improved the deformability and extension of the LDPE/NR/WHF$_{NaOH}$ composites. Furthermore, NaOH-treated WHF showed improved interfacial adhesion with the LDPE/NR phases, resulting in reduced ductility of the composites.

Figure 4 shows the molar sorption of the LDPE/NR/WHF and LDPE/NR/WHF$_{NaOH}$ composites at different amount of fibers. The molar sorption of the LDPE/NR/WHF and LDPE/NR/WHF$_{NaOH}$ composites decreased with increasing fiber loading. The total NR content decreased with increasing amount of fibers added to the polymer matrix. The fibers tended to block solvent (toluene) intake to the composites and provided high swelling resistance. A similar swelling behavior of the recycled rubber powder-filled NR compounds was also reported by Ismail et al. [23]. The LDPE/NR/WHF composites provided higher molar sorption value than the LDPE/NR/WHF$_{NaOH}$ composites. This result was due to the poor interaction adhesion between the WHF and LDPE/NR matrices, which led to pore
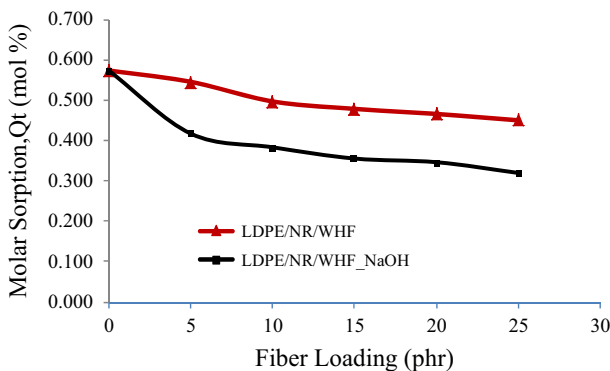

Fig. 4 The effect of alkaline treatment on molar sorption of LDPE/NR/WHF and LDPE/NR/WHF$_{NaOH}$ composites at different amount of fiber

formation and easy penetration of toluene into the composites, resulting in enhanced molar sorption. At similar fiber loadings, the LDPE/NR/WHF$_{NaOH}$ composites exhibited lower molar sorption value than the LDPE/NR/WHF composites because of better interfacial adhesion between the fibers and the matrix in the former and the reduced penetration of toluene into the composites.

Morphology analysis

The SEM morphologies of WHF and WHF$_{NaOH}$ are shown in Fig. 5a, b, respectively. The impurities on the WHF surface were clearly observed. Figure 5b shows that NaOH effectively removed impurities on the WHF surface. Therefore, a cleaner and rougher surface was formed in WHF$_{NaOH}$, which provided more contact area with the matrix and promoted fiber–matrix adhesion.

The SEM micrographs of the tensile fracture surfaces of the LDPE/NR/WHF and LDPE/NR/WHF$_{NaOH}$ composites at different amount of fibers are displayed in Fig. 6. Figure 6a shows that NR was finely and uniformly distributed in the plastic matrix. The LDPE/NR/WHF$_{NaOH}$ composites exhibited better fiber distribution and dispersion than the LDPE/NR/WHF composites at similar fiber loadings. This result indicated better interfacial bonding between the LDPE/NR phases and WHF, resulting in higher tensile strength (Fig. 1). Moreover, the LDPE/NR/WHF$_{NaOH}$ composites displayed rougher surface morphology compared with the LDPE/NR/WHF composites. This characteristic provided better interface adhesion between fibers and matrix. More fiber pull-out and fiber detachments were also observed in the LDPE/NR/WHF composites than those in the LDPE/NR/WHF$_{NaOH}$ composites. Joseph et al. [24] showed that alkali treatment reduced fiber diameter and increased the aspect ratio, which leads to the development of a rough surface morphology and improved fiber–matrix adhesion. Moreover, alkaline treatment improved the hydrophilicity of the fibers, which can create better interfacial reaction with
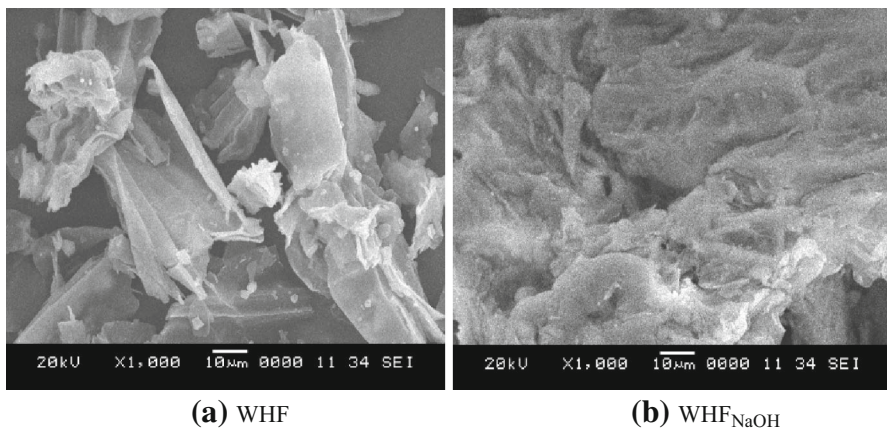

(a) WHF   **(b)** WHF$_{NaOH}$

Fig. 5 The SEM morphology of WHF and WHF$_{NaOH}$

(a) LDPE/NR

Voids

(b) LDPE/NR/WHF-5

(c) LDPE/NR/WHF$_{NaOH}$-5

Rough Surface

Voids

(d) LDPE/NR/WHF-15

(e) LDPE/NR/WHF$_{NaOH}$-15

Rough Surface

Voids

(f) LDPE/NR/WHF-25

(g) LDPE/NR/WHF$_{NaOH}$-25
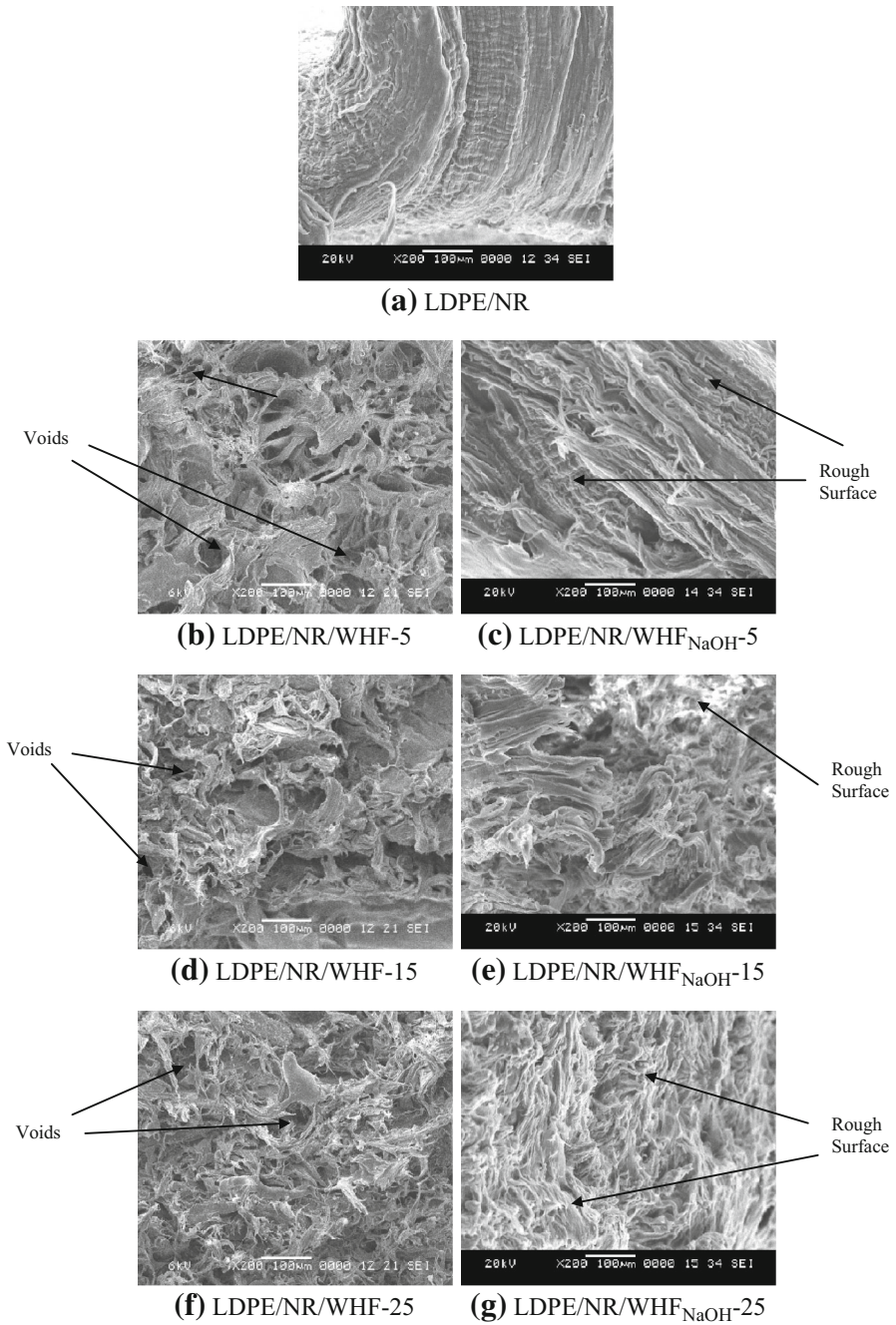
Rough Surface

Fig. 6 The SEM micrographs of tensile fracture surfaces of LDPE/NR/WHF and LDPE/NR/WHF$_{NaOH}$ composites at different amount of fiber

hydrophilic resins and caused less fiber pull-out, as observed in the LDPE/NR/ WHF$_{NaOH}$ composites [25].

Spectroscopy infrared

Figure 7 shows the comparison of the FTIR spectra of WHF$_{NaOH}$ and WHF within the 650–4000 cm^{-1} region. The absorption bands at 3316.86 and 3318.05 cm^{-1} for WHF$_{NaOH}$ and WHF, respectively, correspond to the hydroxyl group (OH). The absorption bands at 2908.67 and 2919.57 cm^{-1} for WHF$_{NaOH}$ and WHF, respectively, may be attributed to CH-stretching vibration. The absorption band at 1732.79 cm^{-1} in WHF is attributed to the carbonyl group (C=O) in hemicellulose. However, the absorption band at 1732.79 cm^{-1} no longer existed in WHF$_{NaOH}$. Similarly, Valadez–Gonzalez et al. reported that alkaline treatment removed hemicellulose, lignin, and pectin in henequen fibers, causing the band to disappear at 1750 cm^{-1} [26]. In addition, the absorption band at 1250.91 cm^{-1} in WHF disappeared after alkaline treatment. This band is assigned to the C-O stretching of the acetyl group of lignin and was removed with NaOH treatment [27]. Absorbance values at 1023.83 and 1024.40 cm^{-1} for the LDPE/NR/WHF$_{NaOH}$ and LDPE/NR/ WHF composites were attributed to C-O formation. The absorption peaks at 837.28 and 842.83 cm^{-1} of both composites are assigned to CH-bending vibration.

The FTIR spectra of the LDPE/NR/WHF$_{NaOH}$ and LDPE/NR/WHF composites are shown in Fig. 8. The absorption intensity ratio decreased after alkaline treatment because of the loss of lignin [28]. In comparison, the spectra of the composites did not show any significant change in the absorption peak for both composites. This
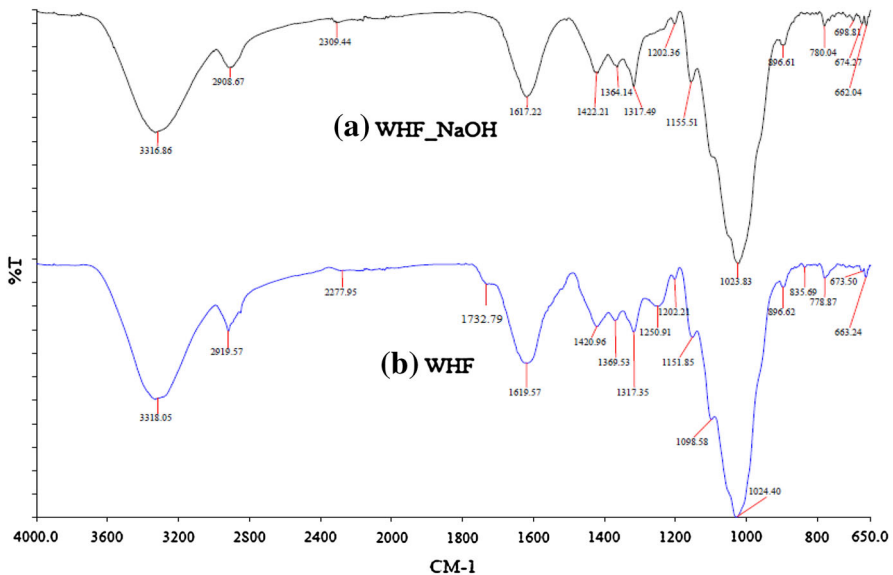

Fig. 7 FTIR spectra for (*a*) WHF$_{NaOH}$ and (*b*) WHF
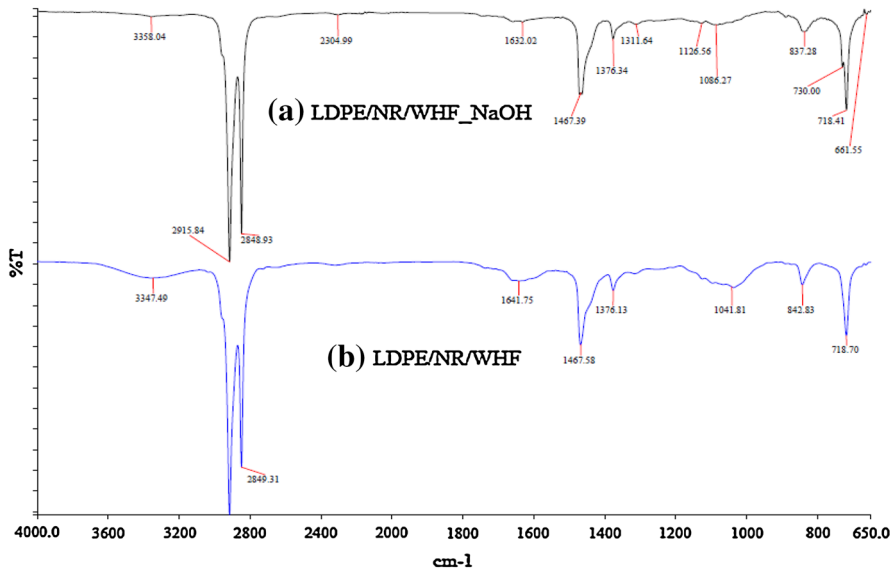
Fig. 8 FTIR spectra for (*a*) LDPE/NR/WHF$_{NaOH}$ and (*b*) LDPE/NR/WHF composites

result could be explained by the matrix (LDPE and NR) adhered to WHF$_{NaOH}$, which caused IR transmission into the composites; as such, no characteristic peak can be clearly observed. The absorption band at the range of 3650–3000 cm^{-1} represents OH stretching. The absorption peaks at 1632.02 and 1641.75 cm^{-1} for the LDPE/NR/WHF$_{NaOH}$ and LDPE/NR/WHF composites, respectively, are attributed to C=O stretching vibration. The absorption band within 1405–1468 cm^{-1} region is attributed to CH$_2$-bending vibration. The bands at 1086.27 and 1041.81 cm^{-1} for the LDPE/NR/WHF$_{NaOH}$ and LDPE/NR/WHF composites are ascribed to C–O vibration from cellulose. The absorption peaks at 837.28 and 842.83 cm^{-1} of both composites are assigned to CH-bending vibration. The illustration of the mechanism underlying the interaction of the LDPE/NR phases with WHF$_{NaOH}$ is shown in Fig. 9.

Thermal properties

Figures 10 and 11 illustrate the DSC thermograms of the LDPE/NR/WHF and LDPE/NR/WHF$_{NaOH}$ composites at different amount of fibers. The thermal parameters of the composites obtained from the DSC thermogram are summarized in Table 2. The melting temperatures (T_m) for the LDPE/NR/WHF and LDPE/NR/WHF$_{NaOH}$ composites decreased with increasing fiber loading. This result could be explained by the composites requiring less heat to melt when fiber content increased. The LDPE/NR/WHF$_{NaOH}$ composites exhibited higher melting temperature than the LDPE/NR/WHF composites at similar fiber loading. This result could be due to alkaline treatment that removed the internal constraint, which leads to better packing of cellulose chains [18, 28]. This closely packed cellulose chain
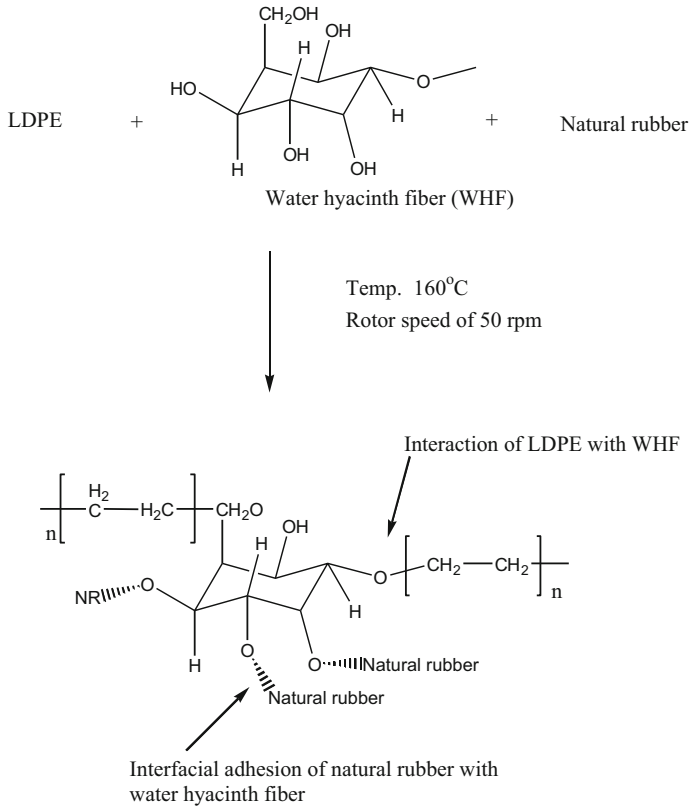
Fig. 9 Illustration of mechanism for the LDPE/NR with alkali-treated water hyacinth fibers (WHF$_{NaOH}$)
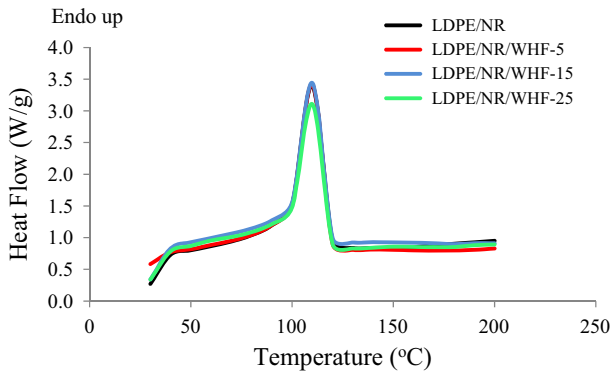

Fig. 10 DSC thermogram of LDPE/NR/WHF composites at different amount of fiber

exhibited higher thermal resistance in combination with the matrix, thereby increasing the melting temperature. In case of crystallinity, both composites demonstrated lower percent crystallinity with increasing amount of fibers added to
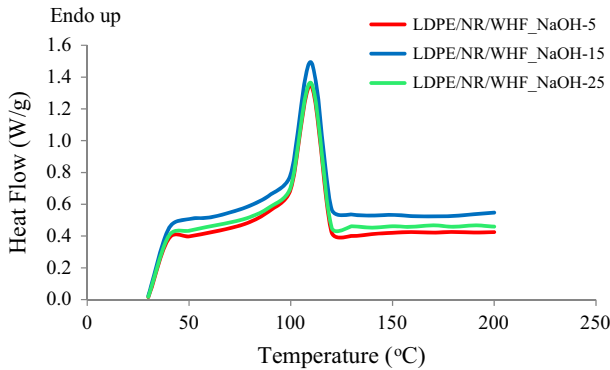
Fig. 11 DSC thermogram of LDPE/NR/WHF$_{NaOH}$ composites at different amount of fiber

Table 2 The thermal parameter for DSC for LDPE/NR/WHF and LDPE/NR/WHF$_{NaOH}$ composites at different amount of fiber

Blend composition	T_m (°C)	Percent crystallinity (%)
LDPE/NR	110.15	28.57
LDPE/NR/WHF-5	110.75	29.67
LDPE/NR/WHF-15	109.78	26.53
LDPE/NR/WHF-25	109.30	21.77
LDPE/NR/WHF$_{NaOH}$-5	110.85	21.91
LDPE/NR/WHF$_{NaOH}$-15	109.99	21.85
LDPE/NR/WHF$_{NaOH}$-25	109.88	19.86

the composites. This reduction of percent crystallinity with the addition of fillers interfered with the chain mobility for crystallization [29]. Furthermore, cellulose, hemicellulose, and impurities were removed after alkaline treatment, resulting in lower percent crystallinity of the LDPE/NR/WHF$_{NaOH}$ composites than that of the LDPE/NR/WHF composite at the same fiber loading.

Thermal degradation

Figures 12 and 13 illustrate the thermogravimetric curves of the LDPE/NR/WHF and LDPE/NR/WHF$_{NaOH}$ composites at different amount of fibers. Table 3 shows the degradation temperatures of 1 and 50 % weight loss, final decomposition temperature, and residue mass for both composites with increasing fiber loading. The initial thermal degradation temperature of the LDPE/NR/WHF composites was lower than the LDPE/NR composite because of gradual evaporation of moisture and some volatile compounds. Moreover, the degradation temperatures for 1 and 50 % weight loss were lower for the LDPE/NR/WHF$_{NaOH}$ composites than those for the LDPE/NR/WHF composites. This finding can be attributed to the loss of cellulose, hemicellulose, lignin, and impurities after alkaline treatment, thereby decreasing the degradation temperature. The removal of natural and artificial impurities in alkali-treated composites reduced residual mass compared with those in the untreated
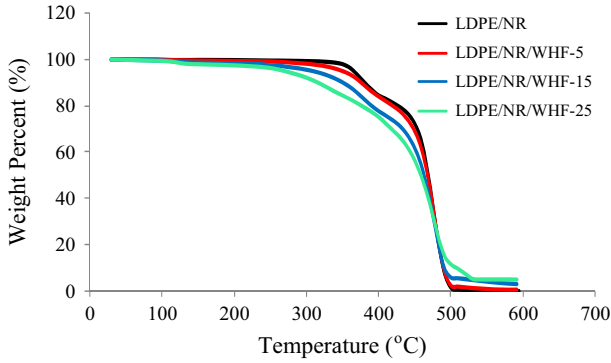
Fig. 12 Thermogravimetric curves of LDPE/NR/WHF composites at different amount of fiber
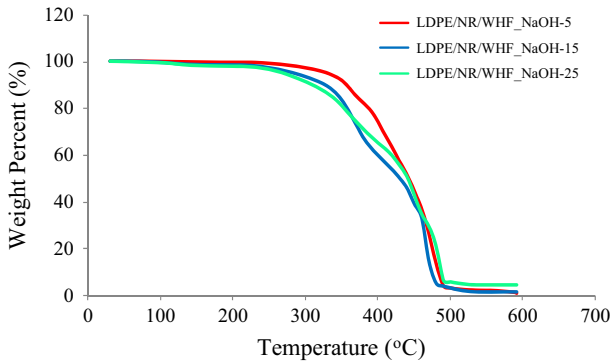

Fig. 13 Thermogravimetric curves of LDPE/NR/WHF$_{NaOH}$ composites at different amount of fiber

Table 3 The temperature of 1 % weight loss, 50 % weight loss, residual mass and final decomposition temperature for LDPE/NR/WHF and LDPE/NR/WHF$_{NaOH}$ composites at different amount of fiber

Blend composition	$T_{-1\ \%wt}$ (^{o}C)	$T_{-50\ \%wt}$ (^{o}C)	Final decomposition temperature (^{o}C)	Residual mass (%)
LDPE/NR	330.12	468.64	594.15	0.021
LDPE/NR/WHF-5	265.89	468.10	591.29	0.675
LDPE/NR/WHF-15	125.97	463.30	591.64	2.563
LDPE/NR/WHF-25	118.36	458.31	591.02	4.784
LDPE/NR/WHF$_{NaOH}$-5	253.57	441.98	591.25	0.615
LDPE/NR/WHF$_{NaOH}$-15	121.17	441.14	591.05	1.187
LDPE/NR/WHF$_{NaOH}$-25	116.79	440.32	590.95	4.133

composites. Hence, alkali-treated fiber decreased the thermal stability of the LDPE/NR/WHF$_{NaOH}$ composites compared with that of the LDPE/NR/WHF composites.

X-ray diffraction (XRD) analysis

The XRD diffractograms of the LDPE/NR/WHF and LDPE/NR/WHF$_{NaOH}$ composites at different amount of fibers are shown in Figs. 14 and 15, respectively. The amount of crystalline phases of the composites reduced after alkaline treatment. These reductions in the crystallinity in the LDPE/NR/WHF$_{NaOH}$ composites confirmed the DSC results. Table 4 indicates the values of 2θ and the average 2θ, which were calculated from the XRD diffractogram, whereas the values and the average interparticle spacing (d) were calculated according to Bragg's Law (Eq. 3). The average interparticle spacing of both composites decreased from 5 to 15 phr fiber loading but slightly increased at 25 phr. This result could be attributed to the good interfacial bonding of the fibers and the matrix at 5 and 15 phr. Further increase in fiber loading caused the composites to form agglomeration, resulting in weak interfacial adhesion, as evidenced in the SEM morphology. Therefore, the average interparticle spacing of the composites increased. Comparison of the LDPE/NR/WHF and LDPE/NR/WHF$_{NaOH}$ composites showed that the value of the average interparticle spacing of the alkali-treated composites was lower than that of the untreated composites. This result could be due to the removal of hemicellulose, lignin, and impurities from the WHF, resulting in the formation of rougher surface. This rougher surface increased the surface area, which provides large area of contact between the fibers and matrix [1]. One of the consequences of the large surface area
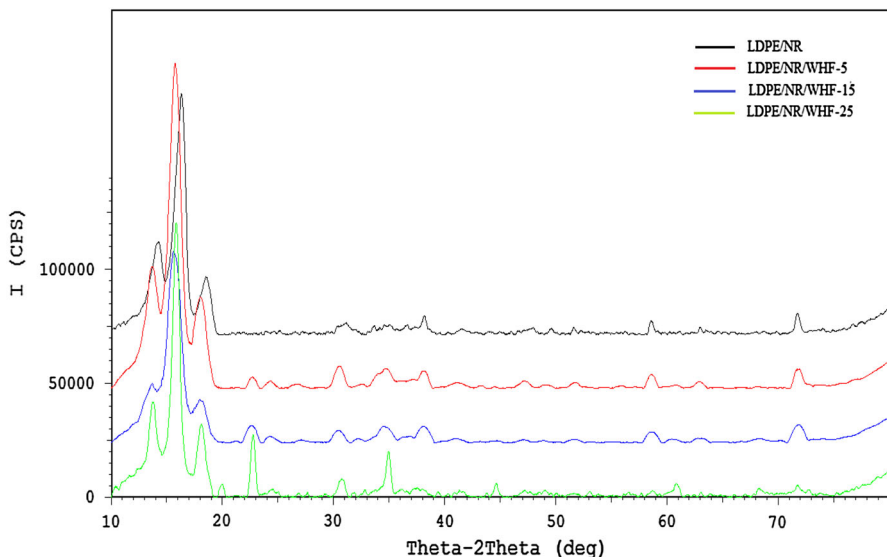

Fig. 14 XRD diffractogram of LDPE/NR/WHF composites at different amount of fiber
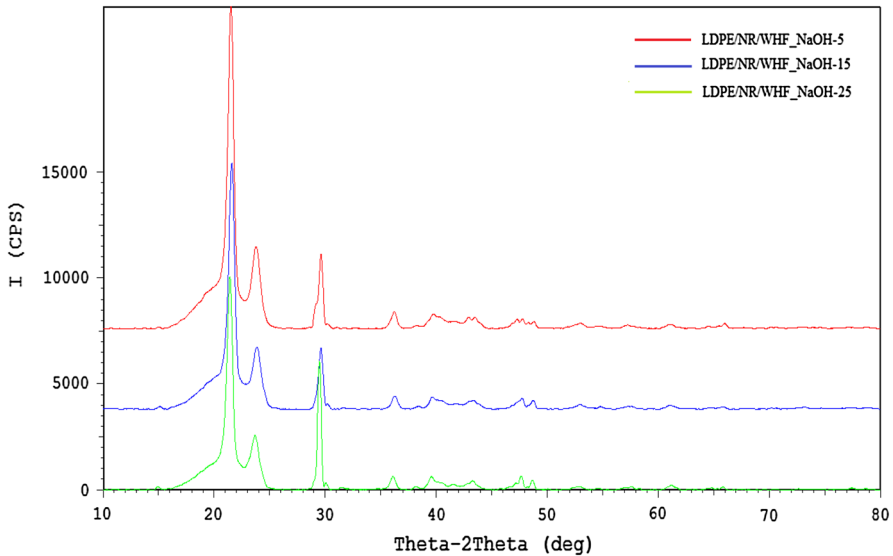
Fig. 15 XRD diffractogram of LDPE/NR/WHF$_{NaOH}$ composites at different amount of fiber

Table 4 Data of interparticle spacing (*d*) for LDPE/NR/WHF and LDPE/NR/WHF$_{NaOH}$ composites at different amount of fiber

Blend composition	Average *d* (nm)
LDPE/NR	0.3580
LDPE/NR/WHF-5	0.3567
LDPE/NR/WHF-15	0.3499
LDPE/NR/WHF-25	0.3738
LDPE/NR/WHF$_{NaOH}$-5	0.3148
LDPE/NR/WHF$_{NaOH}$-15	0.2764
LDPE/NR/WHF$_{NaOH}$-25	0.2788

is improved interfacial adhesion among fibers and matrix, thus reducing interparticle spacing.

Conclusion

Alkaline treatment on WHF improved tensile strength and Young's modulus but reduced ductility and molar sorption in the LDPE/NR/WHF composites. The FTIR results confirmed the removal of hemicellulose, lignin, and impurities in WHF, as evidenced by the disappearance of the absorption bands at 1732.79 and 1250.91 cm^{-1}, which correspond to the carbonyl group (C=O) of hemicellulose and C–O stretching of the acetyl group of lignin. SEM morphological observation showed that alkaline treatment removed the impurities of fibers and provided rough surface, resulting in improved interfacial adhesion between the fibers and the

matrix. Meanwhile, DSC analysis showed higher melting temperature but lower percent crystallinity of the alkali-treated composites than that of the untreated composites. The thermal stability of the composites increased after alkaline treatment. Furthermore, the LDPE/NR/WHF$_{NaOH}$ composites exhibited lower interparticle spacing than did the LDPE/NR/WHF composites because of better interfacial adhesion among the fibers and the matrix.

References

1. Herrera-Franco PJ, Valadez-Gonzalez AA (2005) Study of the mechanical properties of short natural-fiber reinforced composites. Compos Part B Eng 36:597–608
2. Moorhead K, Reddy K, Graetz D (1988) Water hyacinth productivity and detritus accumulation. Hydrobiologia 157:179–185
3. Bhattacharya A, Kumar P (2010) Water hyacinth as a potential biofuel crop. Electron. J Environ Agric Food Chem 9:112–122
4. Malik A (2007) Environmental challenge vis a vis opportunity: the case of water hyacinth. Environ Int 33:122–138
5. Fernández OA, Sutton DL, Lallana VH, Sabbatini MR, Irigoyan JH (1990) Aquatic weeds problems and management in South and Central America. In: Pieterse AH, Murphy KJ (eds) Aquatic weeds. The ecology and management of nuisance aquatic vegetation. Oxford Science Publications, New York, pp 406–425
6. Epstein P (1998) Weeds bring disease to the east African waterways. Lancet 351:577
7. Opande GO, Onyango JC, Wagai SO (2004) Lake victoria: the water hyacinth (*Eichhornia crassipes* [Mart.] Solms), its socio-economic effects, control measures and resurgence in the Winam gulf. Limnol-Ecol Manag Inland Waters 34:105–109
8. Patel V, Desai M, Madamwar D (1993) Thermochemical pretreatment of water hyacinth for improved biomethanation. Appl Biochem Biotech 42:67–74
9. Mantia FL, Dintcheva NT, Morreale M, Vaca-Garcia C (2004) Green composites of organic materials and recycled post-consumer polyethylene. Polym Int 53:1888–1891
10. Holbery J, Houston D (2006) Natural-fiber-reinforced polymer composites in automotive applications. JOM 58:80–86
11. Kalia S, Kaith BS, Kaur I (2009) Pretreatments of natural fibers and their application as reinforcing material in polymer composites—a review. Polym Eng Sci 49:1253–1272
12. Kalia S, Dufresne A, Cherian BM et al (2011) Cellulose fibers: cellulose-based bio- and nanocomposites: a review. Int J Polym Sci 2011:1-837875–35-837875. doi:10.1155/2011/837875
13. Bisanda ETN, Ansell MP (1991) The effect of silane treatment on the mechanical and physical properties of sisal-epoxy composites. Compos Sci Technol 41:165–178
14. Goswami P, Blackburn RS, El-Dessouky HM, Taylor J, White P (2009) Effect of sodium hydroxide pre-treatment on the optical and structural properties of lyocell. Eur Polym J 45:455–465
15. Gwon J, Lee S, Chun S, Doh G, Kim J (2010) Effect of chemical treatments of wood fibers on the physical strength of polypropylene based composites. Korean J Chem Eng 27:651–657
16. Karnani R, Krishnan M, Narayan R (1997) Biofiber-reinforced polypropylene composites. Polym Eng Sci 37:476–483
17. Li X, Tabil L, Panigrahi S (2007) Chemical treatments of natural fiber for use in natural fiber-reinforced composites: a review. J Polym Environ 15:25–33
18. Bledzki AK, Gassan J (1999) Composites reinforced with cellulose based fibres. Prog Polym Sci 24:221–274
19. Alawar A, Hamed AM, Al-Kaabi K (2009) Characterization of treated date palm tree fiber as composite reinforcement. Compos Part B Eng 40:601–606

20. Carter HA (1996) The chemistry of paper preservation. Part III. The strengthening of paper. J Chem Educ 73:1160–1165
21. Threepopnatkul P, Kaerkitcha N, Athipongarporn N (2009) Effect of surface treatment on performance of pineapple leaf fiber–polycarbonate composites. Compos Part B Eng 40:628–632
22. Supri AG, Tan SJ, Ismail H, The PL (2011) Effect of poly(methyl methacrylate) modified water hyacinth fiber on properties of low density polyethylene/natural rubber/water hyacinth fiber composites. Polym-Plast Technol 50:898–906
23. Ismail H, Nordin R, Noor AM (2002) Cure characteristics, tensile properties and swelling behaviour of recycled rubber powder-filled natural rubber compounds. Polym Test 21:565–569
24. Joseph K, Mattoso LHC, Toledo RD, Toledo S, Thomas LH, Pothen L, Kala S, James B (2000) Natural fibers reinforced thermoplastic composites. In: Frollini E, Leao AL, Mattoso LHC (eds) Natural polymers and agrofibers composites. USP-IQSC, UNESP and Embrapa, San Carlos, pp 159–202
25. Gomes A, Matsuo T, Goda K, Ohgi J (2007) Development and effect of alkali treatment on tensile properties of curaua fiber green composites. Comps Part A 38:1811–1820
26. Valadez-Gonzalez A, Cervantes-Uc JM, Olayo R, Herrera-Franco PJ (1999) Effect of fiber surface treatment on the fiber–matrix bond strength of natural fiber reinforced composites. Compos Part B 30:309–320
27. Suardana NPG, Piao YJ, Lim JK (2011) Mechanical properties of hemp fibers and hemp/pp composites: effects of chemical surface treatment. Mater Phys Mech 11:1–8
28. Sinha E, Rout S (2009) Influence of fibre-surface treatment on structural, thermal and mechanical properties of jute fibre and its composite. Bull Mater Sci 32:65–76
29. Gwon JG, Lee SY, Chun SJ, Doh GH, Kim JH (2010) Effects of chemical treatments of hybrid fillers on the physical and thermal properties of wood plastic composites. Comps Part A 41:1491–1497